

Wave–current interactions: an experimental and numerical study. Part 1. Linear waves

By G. P. THOMAS†

School of Mathematics, University of Bristol, Bristol BS8 1TW

(Received 15 September 1980)

The interaction between a regular wavetrain and an adverse current containing an arbitrary distribution of vorticity, in two dimensions, is studied using a linear theory. The model is used to predict the wavelength and the particle velocities under the waves and these are found to agree well with experimentally obtained data for a number of current profiles. Surprisingly accurate predictions, for the profiles considered, were also obtained from an irrotational wave–current model in which the constant current has a value equal to the depth-averaged mean of the measured current profile. The changes in the wave amplitude as the current magnitude increases are predicted using an irrotational slowly varying model with good agreement being found between theory and experiment.

1. Introduction

The interaction between a steady rotational current and a regular wavetrain in two dimensions has not been studied extensively for currents containing an arbitrary distribution of vorticity. The main difficulty in attempting an analytical treatment even for linear waves is that the governing equation (the Rayleigh equation of classical stability theory) cannot be solved exactly for general wavenumbers and frequencies unless the vorticity is constant. Accordingly approximations concerning the nature of the wave regime or the current profile are necessary if analytical solutions are sought. The existing analytical work for both linear and finite-amplitude waves, together with the appropriate approximations, is well documented in the major review of Peregrine (1976) and the shorter reviews of Dalrymple (1973) and Thomas (1979*a*).

The difficulties associated with analytical models have necessitated the development of numerical methods to study arbitrary shear flows. For linear waves, Fenton (1973) used an initial-value formulation to study a $\frac{1}{7}$ -power-law current distribution but his method is capable of describing arbitrary shear flows with both periodic and decaying wave modes. Dalrymple (1973) developed a finite-difference model to study finite amplitude wave–current interactions for an arbitrary distribution of vorticity; the method can also be used for linear waves but would be inefficient in this case.

Both Dalrymple (1973) and Peregrine (1976) have stressed that there is an acute shortage of fundamental experimental work to test existing wave–current theories. This has generally been due to practical difficulties experienced in generating uniform laminar currents and regular waves simultaneously in a laboratory wave flume. An assessment of the problems encountered has been made by Shaw & Hutchinson (1978). Among the earliest experiments were those of Yu (1952) who studied the breaking of waves by an opposing current. Sarpkaya (1955, 1957) considered the stability of

† Present address: Department of Mathematical Physics, University College, Cork, Eire.

progressive waves on a turbulent current in an attempt to evaluate the combined influence of viscous shear, turbulent mixing and a non-uniform current distribution. A novel feature of this work, from an experimental viewpoint, is the use of a wave-maker designed using a 'Venetian blind' principle. More recently, van Hoften & Karaki (1976) have measured the interaction between waves and a turbulent current, showing that energy is extracted from the waves and this manifests itself by increased wave attenuation.

For laminar currents, experiments are fraught with difficulties caused by the unwanted intrusion of turbulent influences. Evans (1955) conducted a series of experiments to test Taylor's (1955) analysis of the hydraulic breakwater, obtaining reasonable agreement between theory and experiment. However, Evans notes that the generation of surface currents inevitably resulted in turbulence, the influence of which could not be quantified. Three-dimensional wave-current interactions were studied by Hughes & Stewart (1961), but while the interaction between the waves and a current with a horizontal shear was demonstrated well, problems were experienced with turbulent regions in the flow. In a preliminary report on the present work, Thomas (1979*b*) has shown good agreement between theory and experiment for linear waves on a current with arbitrary shear in two dimensions with great care taken to minimise the turbulent influences. Brevik & Aas (1980) have obtained quantitatively good agreement between theory and experiment for waves on a shear flow, but were hindered by the degree of turbulence in the current.

The analytical, numerical and experimental work described above has essentially been concerned with local flow behaviour. If the current varies over a length scale of several wavelengths then the corresponding modulations in the wave properties can be studied using a slowly varying approach. This enables the change in wave properties, relative to a fixed reference point in the flow, to be obtained from a number of conservation relations. For general wave problems the technique is well summarized by Whitham (1974), but for the special case of linear waves riding on an irrotational steady current in infinitely deep water the appropriate conservation relations were first given by Longuet-Higgins & Stewart (1961). However, little work exists for rotational currents and the theory cannot as yet be used to include arbitrary distributions of vorticity; the only available relations are those of Jonsson, Brink-Kjaer & Thomas (1978) for flows containing constant vorticity, i.e. where the current varies linearly with depth.

The present work is concerned with interaction between a regular linear wavetrain and a steady adverse shear current in two dimensions. An inviscid numerical model similar to that of Fenton (1973), but more suited to the handling of experimentally obtained data, is developed in §2. The experimental facility and procedure are described in §3. A comparison between theory and experiment is made in §4 and shows very good agreement for both the wavelengths and the velocity profiles. The predictions of a simple analytical model describing the irrotational interaction between a linear wavetrain and a constant current, having a value equal to the depth-averaged mean of the measured current, are also compared with the experimental data and surprisingly good agreement is found. In §5 the irrotational slowly varying theory is used to predict the amplitude variations as the current becomes stronger; although the slowly varying theory is not strictly applicable it is shown to furnish good agreement with the measured wave amplitudes.

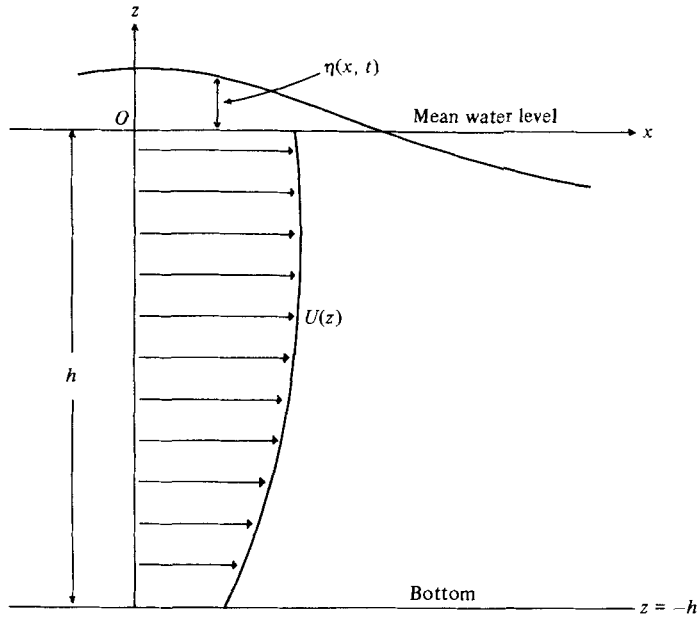


FIGURE 1. Definition of the co-ordinate system.

2. Theory

The co-ordinate system is shown in figure 1. The origin is taken to lie in the mean water level with the z axis pointing vertically upwards and the x axis in the direction of wave propagation. For the flows considered here there are no variations perpendicular to the Oxz plane, so changes in the current occur solely due to upwelling or downwelling from below, and the waves do not undergo refraction.

In the linear theory the surface elevation $\eta(x, t)$ is sinusoidal and can be written

$$\eta(x, t) = a \cos(\kappa x - \omega t), \tag{2.1}$$

where a is the surface wave amplitude, κ the wavenumber and ω the absolute wave frequency. The total velocity field $(u_T(x, z, t), w_T(x, z, t))$ is represented as a superposition of a time-independent current term and wavelike first-order term

$$\left. \begin{aligned} u_T(x, z, t) &= U(z) + u(z) \cos(\kappa x - \omega t), \\ w_T(x, z, t) &= w(z) \sin(\kappa x - \omega t), \end{aligned} \right\} \tag{2.2}$$

where $U(z)$ corresponds to the current profile when no waves are present.

From Peregrine (1976, equation (4.8)) the depth variation $w(z)$ of the vertical wavelike velocity satisfies the Rayleigh equation of classical inviscid stability theory

$$\frac{d^2 w}{dz^2} - \left[\kappa^2 - \frac{\kappa}{\omega - \kappa U} \frac{d^2 U}{dz^2} \right] w = 0 \tag{2.3}$$

in the flow region $-h < z < 0$. The boundary conditions to be satisfied by $w(z)$ are

$$w(z) = 0 \quad \text{on} \quad z = -h, \tag{2.4 a}$$

$$\left. \begin{aligned} (\omega - \kappa U)^2 \frac{dw}{dz} + \kappa(\omega - \kappa U) w \frac{dU}{dz} - g\kappa^2 w &= 0 \\ w(z) &= a(\omega - \kappa U) \end{aligned} \right\} \text{on} \quad z = 0, \tag{2.4 b}$$

where the first surface boundary condition is the dispersion relation and the second is the kinematic free-surface condition.

The quantities ω , a and h , together with the function $U(z)$, can be regarded as known from either experimental specifications or measurements, so the system (2.3) and (2.4) needs to be solved for κ and $w(z)$. When these unknowns have been found the depth-varying component of the wavelike horizontal velocity $u(z)$ can be obtained from the continuity equation

$$u(z) = \frac{1}{\kappa} \frac{dw}{dz}, \quad (2.5)$$

which is valid at all points in the fluid.

The system defined by (2.3) and (2.4) cannot be solved analytically for general wavenumbers and frequencies unless $d^2U/dz^2 = 0$, corresponding to either a depth independent current or one which varies linearly with depth. Solutions for more general profiles are obtainable for stationary waves or if long- or short-wave approximations are applied; in each of these cases the existing analytic solutions are well documented by Peregrine (1976, §IVB).

For the purposes of the present work it is necessary to resort to numerical solution of (2.3) and (2.4). The first step is to formulate the problem as an initial-value one which is more amenable to numerical treatment. Define y , $\phi(y)$ and $U_1(y)$ as follows

$$\phi(y) = w(z)/h \frac{dw}{dz}(-h), \quad y = \frac{z}{h}, \quad U_1(y) = U(z) \quad (2.6)$$

and substitute into (2.3) and (2.4 *a, b*). The Rayleigh equation becomes

$$\frac{d^2\phi}{dy^2} - \left[(\kappa h)^2 - \frac{\kappa}{\omega - \kappa U_1(y)} \frac{d^2 U_1}{dy^2} \right] \phi = 0 \quad \text{in} \quad -1 < y < 0, \quad (2.7)$$

with the initial conditions

$$\phi(-1) = \frac{d\phi}{dy}(-1) = 0. \quad (2.8a)$$

The surface condition corresponding to the dispersion relation is

$$F(\kappa) = \left\{ 1 - \frac{\kappa U_1}{\omega} \right\}^2 \frac{d^2\phi}{dy^2} + \frac{\kappa}{\omega} \left\{ 1 - \frac{\kappa U_1}{\omega} \right\} \phi \frac{dU_1}{dy} - \frac{gh}{\omega^2} \phi = 0 \quad \text{on} \quad z = 0. \quad (2.8b)$$

This initial-value problem, with the condition (2.8 *b*), has been considered previously by Fenton (1973) who presented numerically-obtained solutions for the particular profile $U_1(y) = U_0 \cdot (1+y)^{\frac{1}{2}}$. Fenton's method of solution regarded κh and $\kappa U_0/\omega$ as known parameters; $\phi(y)$ was determined from the initial-value problem and then the surface condition yielded the non-dimensional phase velocity $c/(gh)^{\frac{1}{2}}$, where $c = \omega/\kappa$. In the present case the known quantities are ω , h and $U_1(y)$, so that it is not convenient to specify κh and $\kappa U_1(0)/\omega$ as predetermined fixed parameters; consequently Fenton's method is not directly applicable. It is simpler to regard the system (2.7) and (2.8 *a*) as one with an unknown function $\phi(y)$ and an unknown quantity κ , related by the surface condition (2.8 *b*).

Suppose the value $\kappa = \kappa_1$ is fixed *a priori*. With this value of κ equation (2.7), subject to the initial conditions (2.8 *a*), is readily solved by use of a standard computer library Runge-Kutta routine and $F(\kappa_1)$ is then obtained from (2.8 *b*). If another value

$\kappa = \kappa_2$ is chosen, $F(\kappa_2)$ can be found similarly. By choosing κ_1 and κ_2 such that $F(\kappa_1) \cdot F(\kappa_2) < 0$ the solution to $F(\kappa) = 0$ can be found iteratively using the modified method of false position for a value of κ between κ_1 and κ_2 . When $F(\kappa) = 0$ is satisfied then we have $\phi(y)$ also, since this is obtained in the derivation of $F(\kappa)$. Care must be taken to ensure that if more than one zero exists then the one which is found is physically meaningful; this depends on the choice of the initial guesses κ_1 and κ_2 . In practice the algorithm works well with the quantities κ_1 and κ_2 defined by

$$\left. \begin{aligned} \omega^2 &= g\kappa_1 \tanh \kappa_1 h, \\ (\omega - \kappa_2 U_{\max})^2 &= g\kappa_2 \tanh \kappa_2 h, \end{aligned} \right\} \quad (2.9)$$

with U_{\max} being the maximum adverse current. The value κ_1 corresponds to the irrotational zero-current wavenumber for the wave frequency and water depth as used in the experiments; κ_2 is the analogous wavenumber for irrotational waves running against the constant adverse current U_{\max} . The choice of κ_1 and κ_2 was deduced from wavelength considerations which suggest $\kappa_1 < \kappa < \kappa_2$.

With $\phi(y)$ and κ known the numerical problem can be regarded as solved. The quantities to be determined are the wavelength $\lambda = 2\pi/\kappa$ and the wavelike velocity profiles $u(z)$ and $w(z)$. In terms of $\phi(y)$ and κ , $w(z)$ is given by (2.6) and the second relation in (2.4*b*) as

$$w(z) = \frac{\phi(y)}{\phi(0)} a(\omega - \kappa U(0)), \quad (2.10)$$

with $u(z)$ then determined from (2.5).

The function $U(z)$ (or equivalently $U_1(y)$) is regarded as known, but is in practice known only as a set of (typically twenty) data points. Accordingly an analytical or numerical approximation to give $U(z)$ from the basic data is required and this must be sufficiently accurate so as to provide good approximations to both dU/dz and d^2U/dz^2 as well as to $U(z)$. Cubic spline interpolation functions were used to fit the data for $U(z)$; these satisfy the above accuracy requirements and have the additional advantage that a standard computer library procedure is usually available.

3. The experimental facility and procedure

(a) Experimental facility

The experimental programme was carried out in the Hydraulic Laboratory of the Department of Civil Engineering, University of Bristol. A longitudinal schematic section of the flume used for the experiments is shown in figure 2; this flume also has a wind generation facility, but this was not used and so is not illustrated.

The flume has an overall length of approximately 27 m. The working section between the beach and the paddle has a uniform width of 0.72 m and a horizontal floor. Behind the beach the flume width is approximately twice that of the working section and is so designed to act as a stilling basin which minimizes fluctuations introduced by the pump when currents are used.

Waves are generated by a hydraulically driven flat paddle board which can be controlled by either a regular signal generator or a pre-recorded random signal as required. This type of wavemaker has been shown by Ursell, Dean & Yu (1960) to be efficient over a wide range of wave frequencies, including those encountered in this

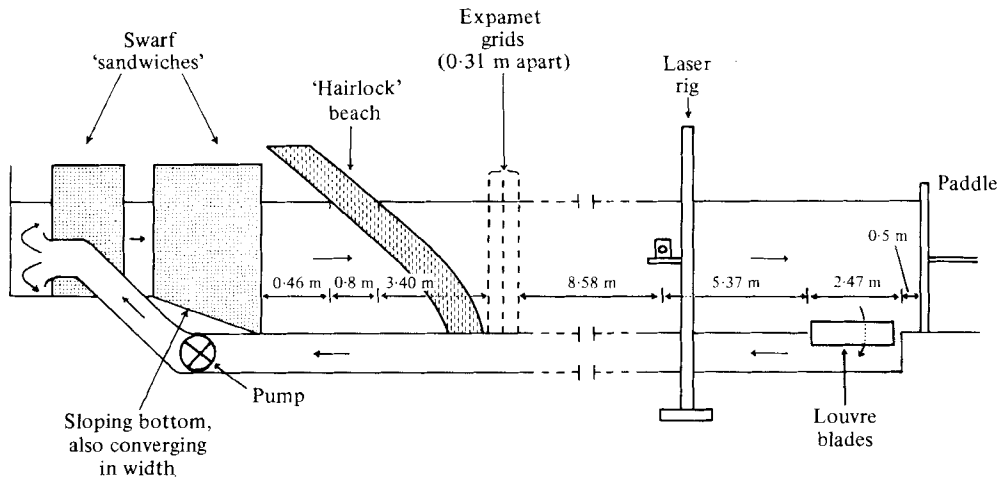


FIGURE 2. Schematic section of the wind-wave-current flume in the Hydraulics Laboratory, Department of Civil Engineering, University of Bristol. The drawing is not to scale and does not show the wind facility.

study, in the generation of regular sinusoidal waves within the linear wave regime. Unwanted wave reflections are removed by a beach constructed of three thicknesses of 'Hairlock' bound in an 'expamet' sandwich. The beach is 5.5 m in length and of adjustable slope, usually chosen to provide maximum beach length (and efficiency) at the required water depth; the lowest portion of the beach was contoured parabolically in the manner shown in figure 2. Following Ursell, Dean & Yu (1960, equation (7.1)), the beach reflection coefficient is defined as the ratio of the reflected wave height to the incident wave height; for the wave conditions in the experiments described here the reflection coefficient, for waves only, was found to be less than 2%. This value was determined from careful measurements of the variation in wave height along the length of the flume, with the louvres closed and the expamet grids removed.

The current motion is driven by a pump with an adjustable motor and provides a re-circulatory flow in which the current in the flume is adverse to the direction of wave propagation. Water is removed from the flume over a distance of approximately 2.5 m in front of the paddle and travels, via a return duct under the main floor of the flume, to be pumped into the stilling basin behind the beach. A feature of the facility is that for experiments which do not require currents, the louvre blades can be closed to provide a flume with a uniformly horizontal floor. There are five identical louvre blades and each can rotate about a horizontal axis in the flume floor; when open the blades are vertical and parallel to the sides of the flume, thus presenting very little flow obstruction.

The theory requires the current to be laminar and this necessitates maintaining the level of turbulence in the current within acceptable bounds. The strategy is to diffuse as much of the large scale turbulence as possible in the current; before precautions were taken deviations from the mean current velocity were of the order of 40% of the mean. Small-scale high-frequency turbulence is not an insurmountable problem since its influence can be removed by averaging over a sufficiently large number of wave cycles.

The main generative sources of large-scale turbulence are readily identifiable: the current is turned through 180° at the bell mouth from the pump into the stilling basin and then flows through both a convergent channel and a thick beach before moving down into the working section of the flume. Two principal steps were taken to reduce this large-scale turbulence. Firstly, two substantial 'sandwiches' of fine stainless swarf (lathe turnings), of thickness 0.6 m and 1 m, were placed directly after the pump bell mouth and in the convergent channel respectively; these are shown in figure 2. Tests conducted with the beach removed showed that these devices provided a particularly effective mechanism for dispersing the large-scale turbulence. Secondly, three 'expamet' grids were placed immediately in front of the beach at roughly 0.3 m intervals to reduce the turbulence introduced by streaming through the beach; the grid size was chosen to be sufficiently large (having an open area of 60 %) for the wave motions not to experience appreciable reflection when the current flowed and fortunately this proved to be so in practice. The introduction of these two types of current filter reduced the scale of the turbulence to an acceptable level; typical deviations at the measuring point were less than 4 % of the mean velocity and hence were considered 'removable' by an averaging process.

The wave and current velocities are measured using laser-Doppler anemometry (LDA). The laser is a Spectra-Physics 124A(15mw) and the transmitting, receiving and processing optical units are contained in a modified Mark 1 DISA system. The manufacturer's accuracy specification for this LDA system is an error of less than 1 % of the true value. Wave heights and profiles are measured using resistance type gauges built to the design developed at the Hydraulics Research Station, Wallingford. The oscillatory LDA and wave probe output is analysed on-line by a S.E. Labs Model SM2002A Transfer Function Analyser, which is also used to generate the regular sinusoidal waves. This resolves the input signal into a nine-harmonic Fourier series, averaged over an arbitrarily prescribed number of wave cycles. The non-oscillatory LDA output, corresponding to the mean current, is evaluated using an averaging microprocessor voltmeter.

(b) *Experimental procedure*

The following procedure was adopted in each of the experiments.

The pump motor was set to the required speed and the water depth adjusted to give the desired value when measured immediately in front of the paddle (this is essentially a region of still water when waves are not generated).

The horizontal current profile $U(z)$ was measured at a number of elevations (typically twenty), spaced uniformly over the greater part of the water depth. It was not possible with the experimental rig used to measure within 45 mm of the bottom of the flume, so no data points were obtained from this region. Additionally a greater density of points was used near the air-water interface since this was where the strongest shear generally occurred. At each measuring point the mean horizontal current was found by averaging the LDA output signal over a sufficiently long period, typically of the order of 120 secs. The maximum deviation from the mean was also noted to ensure that the turbulence fluctuations remained within the bounds described earlier.

A steady wave train was then generated at a prescribed frequency and of an

amplitude controlled by the stroke of the sinusoidal paddle motion. The first harmonic component of the horizontal velocity was measured at a number of points (usually twelve), with the signal averaged over 100 wave cycles; for a wave frequency of 0.8 Hz this is approximately the same time as used in obtaining the mean current. The averaged first harmonic component of the surface elevation was determined in a similar manner. Higher harmonics were obtained for both the velocity and surface elevation measurements to ascertain that the motion remained within the linear wave regime. It was not felt necessary to measure both the vertical and horizontal components of the oscillatory velocity at each measuring point, since both are predicted by the numerical model; initial tests showed that the model predicted each to the same degree of accuracy and the continuity equation (2.5) provided excellent agreement between the two velocity components.

Finally the wavelength was determined by placing two wave probes so that their output signals were exactly in phase, this occurs whenever the probes are an integral number of wavelengths apart and the first such position, i.e. one wavelength apart, was sought.

From each experiment the frequency ω , water depth h , wave amplitude a and fundamental current distribution $U(z)$ are either specified or measured and then used as input to the numerical model. The theoretical velocity profiles obtained can then be compared with those measured in the experiment.

4. Results

In the series of experiments described here the water depth immediately in front of the paddle was maintained at 0.57 m, the wave frequency was specified to be 0.8 Hz and the same paddle displacement was always used to generate the waves. Data was obtained for a number of current profiles, and the corresponding wave-current interaction, with the depth-averaged current velocity lying between zero and approximately 0.25 m s^{-1} . The upper limit on the adverse current velocity was governed by the capacity of the pump motor and not by physical considerations – it is perhaps worth noting that under this set of conditions, the irrotational linear wave theory predicts wave reflection when the adverse current is of the order of 0.45 m s^{-1} , which is well outside the present range of interest.

Although the water depth immediately in front of the paddle was kept constant throughout the series of experiments, the mean water depth in the interaction region varied slightly with different currents due to higher-order effects (usually referred to as 'set-up' or 'set-down'). These have been determined to second order by Jonsson *et al.* (1978, equation (37)) for the case of a linear current profile and can essentially be regarded as the sum of second order wavelike terms and the classical hydraulic velocity head. The wavelike terms do not appear in the linear theory used here since they are of second order, but it remains to confirm that the hydraulic head can be justifiably ignored. The hydraulic velocity head increases in magnitude as the current increases and for the strongest current considered Jonsson's exact expression yielded a value of 2 mm, which is $\simeq 0.35\%$ variation in the depth and can be regarded as a genuine second-order quantity.

The measured velocities and corresponding theoretical predictions are presented graphically in figures 3–7 as a sequence in which the current is an increasing quantity.

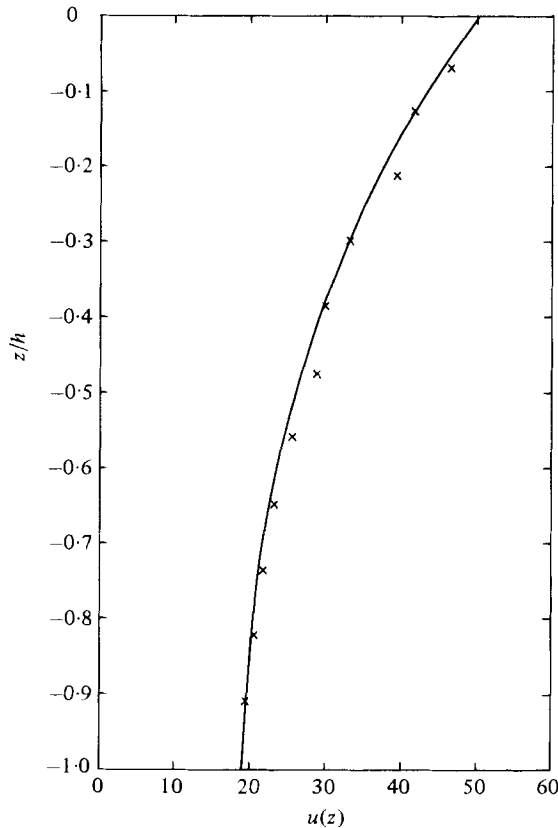


FIGURE 3. Comparison between theory and experiment for the amplitude $u(z)$ (mm s^{-1}) of the wavelike horizontal particle velocity under a regular linear wavetrain in otherwise still water. The physical properties of the wavetrain are given in table 1. —, the predicted profile; \times , experimental data.

In each of the figures the experimental data is shown by a cross and a predicted profile by a solid line; the mean value of the current, when appropriate, is illustrated by a line composed of alternate dashes and dots.

Figure 3 corresponds to the case where there is zero current, so the predicted profile is given by the usual irrotational linear wave theory for waves propagating through otherwise still water. This special case is included as it provides two fundamental reference levels. Firstly, it can be used to relate any of the quantities resulting from the wave-current interaction, such as wavelength or wave velocity, to its value when no current is present. Secondly, it illustrates the case in which experimental data could be expected to furnish the best agreement with theory and hence can be used to provide a reference level for the accuracy of the measuring system.

Good agreement is generally seen to exist between the measured and predicted velocities. The mean discrepancy between the theoretical curves and the measured velocity data is of the order of 4%, corresponding to an error of 1.6 mm s^{-1} when the velocity is 40 mm s^{-1} .

The agreement is poorest in two readily identifiable regions: near to the surface for the weakest current (figure 4) and close to the bed for the stronger currents (figures 6

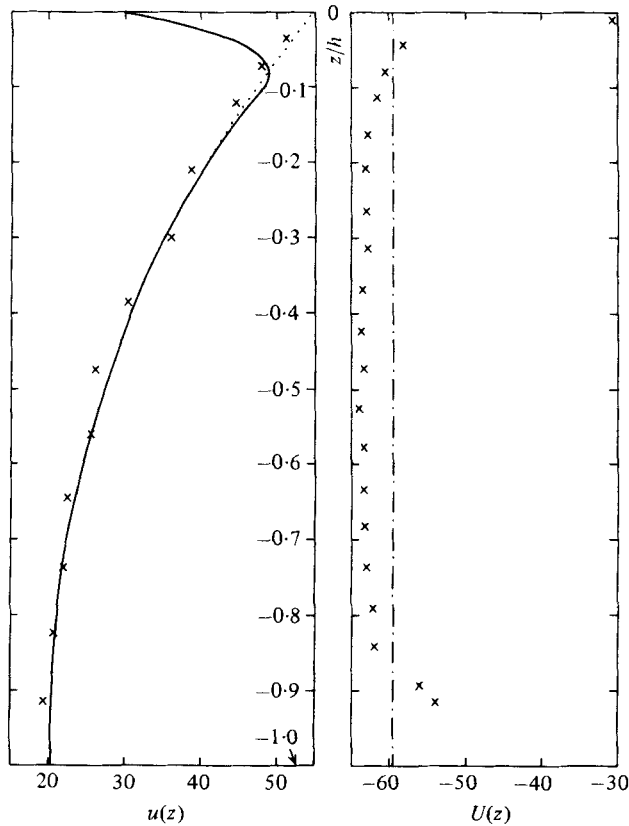


FIGURE 4. Comparison between theory and experiment for the amplitude $u(z)$ of the wavelike horizontal particle velocity under a regular linear wavetrain interacting with the horizontal current $U(z)$. All velocities are measured in mm s^{-1} and the physical properties of the system are given in table 1. —, the predicted profile; \times , experimental data; - - -, the value of the depth-averaged current $\bar{U} = 59.7 \text{ mm s}^{-1}$; ..., the predicted profile using the irrotational mean-flow model.

and 7). From figure 4 the surface discrepancy is seen to be associated with a particularly strong shearing of the water surface layers. In the latter case the source of trouble is not the shear layer at the bed but is instead due to a jet of water which streams through a weak point in the beach construction and becomes more pronounced as the flow becomes faster; the hypothesis of the jet being generated at the beach was confirmed by measurement of current profiles with the beach removed. Such a region of flow could be associated with an instability mechanism (since the profile contains an inflection point) but this was not observed, possibly because the length scale over which the instability could manifest itself was not sufficiently long, but more likely due to small-scale turbulent diffusive processes preventing the growth of such an instability.

This maximum disparity occurs in regions where the rate of shear of $U(z)$ and dU/dz is most rapid and consequently where the current becomes difficult to model numerically. Although the spline fits the experimental data well, its first derivative between any two adjacent knots is quadratic and hence its second derivative is linear in z . Thus the input to the numerical model is in some sense a smoothed form

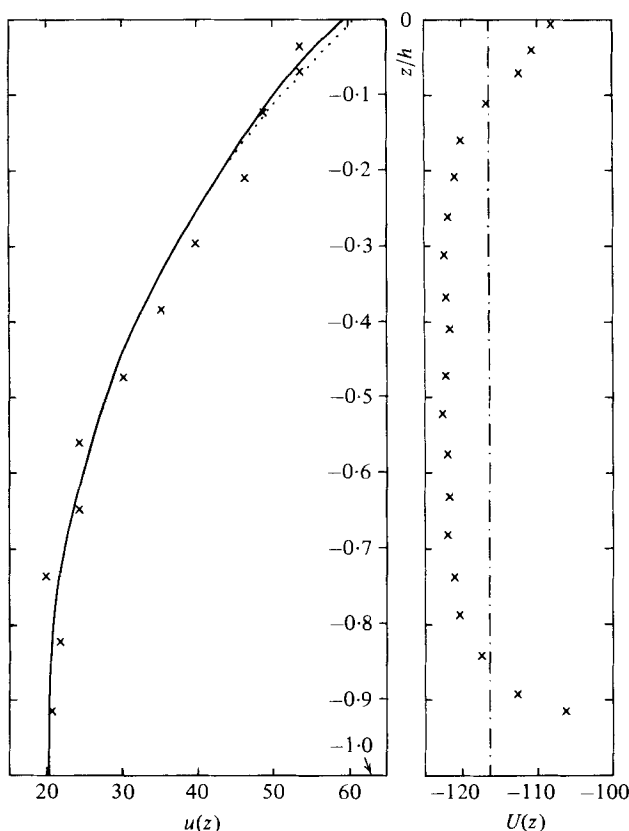


FIGURE 5. As for figure 4, with $\bar{U} = 116.2 \text{ mm s}^{-1}$.

of the data and least accurate in regions of greatest shear, which is then reflected in the predicted velocity profiles. The situation could be improved by the insertion of more data points and more knots in the spline in the regions of greatest shear but this would require considerably more experimental time and a detailed *a priori* knowledge of the current profile.

The influence of the current on the wavelength and wave amplitude is shown in table 1. The strength of the interaction is illustrated by the fact that the measured wavelength λ_m at the maximum current velocity considered (figure 7) has decreased by approximately 19% of its value when no current is present. The corresponding measured increase in wave amplitude is 31% and the magnitude of the maximum predicted horizontal wavelike component, from figures 3 and 7, increases by 37%.

The agreement between the predicted wavelength λ_p and the measured wavelength λ_m is seen to be generally very good with the poorest agreement ironically being for the lowest currents, where it would be expected to be best. For the data in table 1 the maximum value of $|\lambda_m - \lambda_p|$ is $< 0.8\% \times \lambda_p$ with the mean error being $< 0.5\% \times \lambda_p$.

A further quantity presented in table 1 is $\lambda_{\bar{U}}$. This is the wavelength of an irrotational linear wavetrain interacting with the depth-independent (adverse) current \bar{U} and is obtained from the usual irrotational dispersion relation

$$(\omega - \kappa \bar{U})^2 = g\kappa \tanh \kappa h, \quad \lambda_{\bar{U}} = \frac{2\pi}{\kappa} \quad (4.1)$$

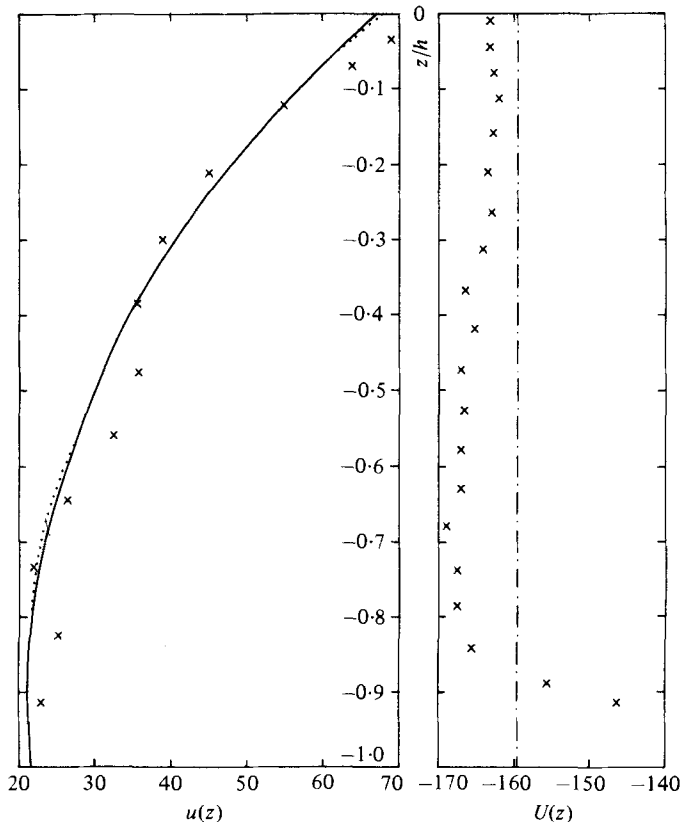


FIGURE 6. As for figure 4, with $\bar{U} = 159.8 \text{ mm s}^{-1}$.

with \bar{U} (the depth averaged mean current) determined from the cubic spline representation of the current data. Surprisingly good agreement is seen to exist between λ_m and $\lambda_{\bar{v}}$, with the errors between the two being of the same order of magnitude as between λ_m and λ_p .

The close proximity enjoyed by λ_m , λ_p and $\lambda_{\bar{v}}$ for the current profiles considered here shows how remarkably good irrotational wave theory can be for wavelength prediction, even in the presence of pronounced, though narrow, shear layers in the current near the flume bottom and the free surface. Of obvious interest is how well the irrotational mean current model can predict the wavelike velocity components.

The appropriate form for the horizontal velocity component $u(z)$ in the irrotational model is

$$u(z) = \frac{ag\kappa}{\omega - \kappa\bar{U}} \frac{\cosh \kappa(z+h)}{\cosh \kappa h} \quad (4.2)$$

with κ determined from (4.1). This can easily be used to predict the measured velocity profiles presented in figures 4-7. Agreement between (4.2) and the experimental data is generally very good for each of the current profiles over almost all of the water depth; this can be seen from figures 4-7, where the dotted line indicates the prediction of (4.2) and appears only where it differs noticeably from the prediction of the numerical model. The main discrepancies are close to the surface in figures 5 and 7, and in

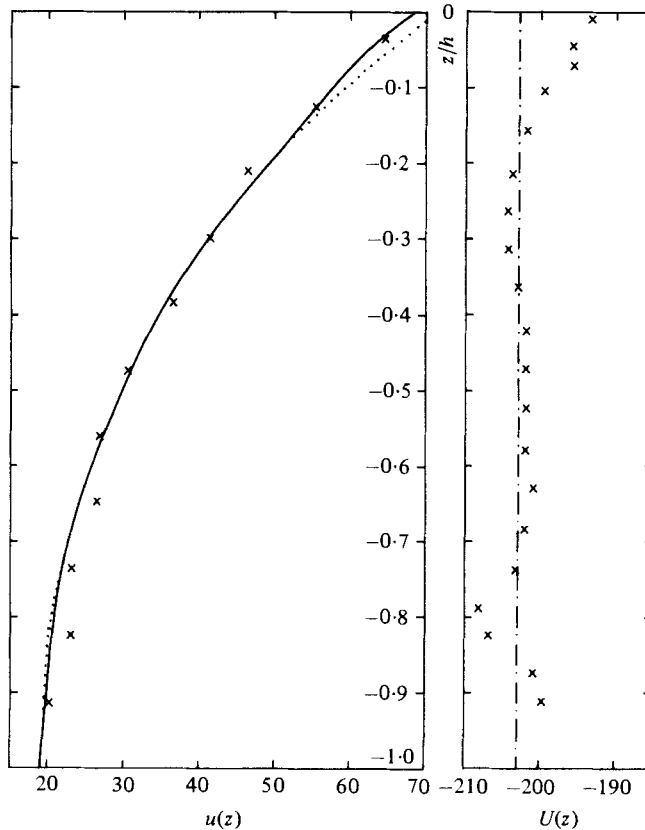
FIGURE 7. As for figure 4, with $\bar{U} = 203.0 \text{ mm s}^{-1}$.

Figure	\bar{U}	λ_p	λ_m	$\lambda_{\bar{U}}$	a_m
3	0	2.246	2.261	2.246	9.18
4	59.7	2.127	2.143	2.125	9.96
5	116.2	2.004	2.007	2.005	10.61
6	159.8	1.902	1.896	1.907	11.63
7	203.0	1.816	1.820	1.806	12.02

TABLE 1. The physical properties of the wave-current interactions illustrated in figures 3–7. The quantity \bar{U} , measured in mm s^{-1} , is the depth-averaged adverse current velocity obtained from the cubic spline interpolation to the current data. The wavelengths λ_p and λ_m (measured in metres) are the predicted and measured values of the wavelengths; $\lambda_{\bar{U}}$ is the wavelength prediction from equation (4.1). Wave amplitudes are denoted by a_m and are measured in millimetres.

the region of the bottom jet in figures 6 and 7. These occur where the irrotational model fails to include the influence of the shear. However, for the results shown in figure 4 the irrotational model is more accurate than the numerical model close to the water surface, largely because the irrotational mean current formulation is relatively insensitive to the nearest current measurement to the surface.

In the experimental results presented above, the frequency, water depth and paddle displacement are all fixed parameters. This choice enables the experimental

data to be used in the next section to study the slowly-varying properties of the flow. Similar experiments were also carried out with different values for these parameters and a comparable degree of agreement between theory and experiment to that shown above was obtained, provided that the waves remained within the linear regime.

5. Slowly varying properties of the flow

The results presented in table 1 show the measured amplitude variation with the current, but the linear theory used to predict the local wave properties does not provide an immediate mechanism for predicting the amplitude variation. Accordingly an alternative approach is required to relate the amplitude variation to the appropriate change in the current properties.

The approach usually adopted to consider such amplitude variations is to assume that the flow properties are slowly varying, i.e. that any changes in the local properties of a steady wavetrain occur over a length scale of several wavelengths. In the present case this is equivalent to the assumption that variations in the current, which generate the variations in the local wave properties, only occur over the prescribed scale of several wavelengths and a further consequence of this is that there is no reflection (partial or total) of the incident wavetrain due to the horizontal current gradient. The theory for irrotational wave-current interactions of this type was first given by Longuet-Higgins & Stewart (1961) for waves in deep water and can be derived for water of arbitrary depth using the Whitham (1974) theory. For rotational currents little work exists; the most applicable is that of Jonsson *et al.* (1978), who consider the case of a current containing constant vorticity.

The currents used in the experimental programme were essentially constant over the main part of the flume between the expamet grids and the drainage louvres and could justifiably be regarded as locally constant in the measuring region. Thus the current changes over the length of the louvres. This distance is approximately 2.5 m and this must be compared with an incident wavelength of between 1.81 m and 2.61 m. Strictly speaking this change in the current velocity over a scale of $O(\lambda)$ is too short a length scale for valid implementation of the slowly varying theory, but in the absence of a more suitable theory a slowly varying regime is assumed to exist.

From Longuet-Higgins & Stewart (1961) the conservation relation governing the amplitude variation of a linear wavetrain on an irrotational current U in infinitely deep water is

$$\frac{1}{2}a^2(c-U)(c+U) = \text{constant}, \quad (5.1)$$

where c is the phase velocity given by $c = \omega/\kappa$. The current variations are assumed to be generated by upwelling (or downwelling).

This relationship can also be extended to water of finite depth and is presented here in its most general form

$$\frac{E}{\omega - \kappa U} c_g = \text{constant}, \quad (5.2)$$

where $E = \frac{1}{2}\rho g a^2$ is the wave energy density and $c_g = d\omega/\kappa$ is the group velocity. The expression (5.2) is often referred to as the conservation of wave action, following Bretherton & Garrett (1968).

For a particular rotational flow, Jonsson *et al.* (1978) have shown that if the current profile varies linearly with depth the analogue of (5.2) is

$$\frac{E}{\omega - \kappa \bar{U}} c_g = \text{constant}, \quad (5.3)$$

where E still represents the wave energy density but is now a complicated function of the wave amplitude, vorticity and current properties. The quantity \bar{U} is the depth-averaged current velocity as used previously in § 4.

For general rotational currents, there is at present no analogue of (5.3). Accordingly, the choice is between (5.2) and (5.3) as to which would better satisfy the required purpose. Study of the current profiles in figures 3-7 indicates the currents are better described by a constant depth-independent value than by a linear law. This suggests using the following form of (5.2),

$$\frac{a^2}{\omega - \kappa \bar{U}} c_g = \text{constant}. \quad (5.4)$$

The corresponding changes in the wavenumber or wavelength can also be predicted in slowly varying regimes and the appropriate conservation relation for linear waves is simply the local dispersion relation. Since the constant current \bar{U} is used to predict the amplitude variations, to be consistent the same current parameter must be used to study the wavelength variations. The dispersion relation has been given previously as equation (4.1),

$$(\omega - \kappa \bar{U})^2 - g\kappa \tanh \kappa h = 0, \quad (5.5)$$

and the values of λ given by this equation were indicated in § 4 by $\lambda_{\bar{U}}$. The error between $\lambda_{\bar{U}}$ and λ_m (the measured value) has been discussed previously and errors of similar magnitude are intuitively expected between the measured and predicted values of the wave amplitudes.

To use (5.4) and (5.5), it is necessary to specify a reference level to define the constant in (5.4) and to enable a non-dimensionalization of all quantities to be made. The natural choice of reference is to the values which are found when there is zero current. This introduces the quantities a_0 and λ_0 , corresponding to the amplitude and wavelength respectively when no current flows; a_0 takes the measured value given for $\bar{U} = 0$ in table 1 and λ_0 takes the corresponding predicted value (which must be used rather than the measured value since (5.5) must be satisfied). All of the required data is available from table 1. This is presented in a more suitable form in table 2 and is shown graphically in figure 8.

Comparison of the measured and predicted wave amplitudes and wavelengths in table 2 and figure 8 shows good agreement between the two sets of data. The agreement between the measured and predicted values of the wave amplitude is generally better than 2% of the predicted value; the corresponding figure for the wavelength data is 1%. This does not suggest that the wavelength prediction is better than the amplitude prediction since the experimental error must be taken into account, i.e. the amplitude data is non-dimensionalized with respect to the measured value a_0 and must contain an element of experimental error, which is then inherent in the a/a_0 predictions. The same problem does not occur in the wavelength predictions, since λ_0 is a theoretical value and is not dependent upon experimental error.

Figure	\bar{U} (mm s ⁻¹)	Measured	Predicted	Measured	Predicted
		a/a_0	a/a_0	λ/λ_0	λ/λ_0
3	0	1	1	1.007	1
4	59.7	1.085	1.067	0.954	0.946
5	116.2	1.156	1.156	0.894	0.893
6	159.8	1.267	1.242	0.844	0.849
7	203.0	1.309	1.315	0.810	0.804

TABLE 2. The measured and predicted values of the non-dimensional wave amplitude and wavelength. The experimental data is taken from table 1 and the predicted values derived using equations (5.4) and (5.5). In the notation of table 1, a_0 and λ_0 correspond to the values of a_m and $\lambda_{\bar{U}}$ when $\bar{U} = 0$; the measured values a/a_0 and λ/λ_0 correspond to a_m/a_0 and λ_m/λ_0 respectively.

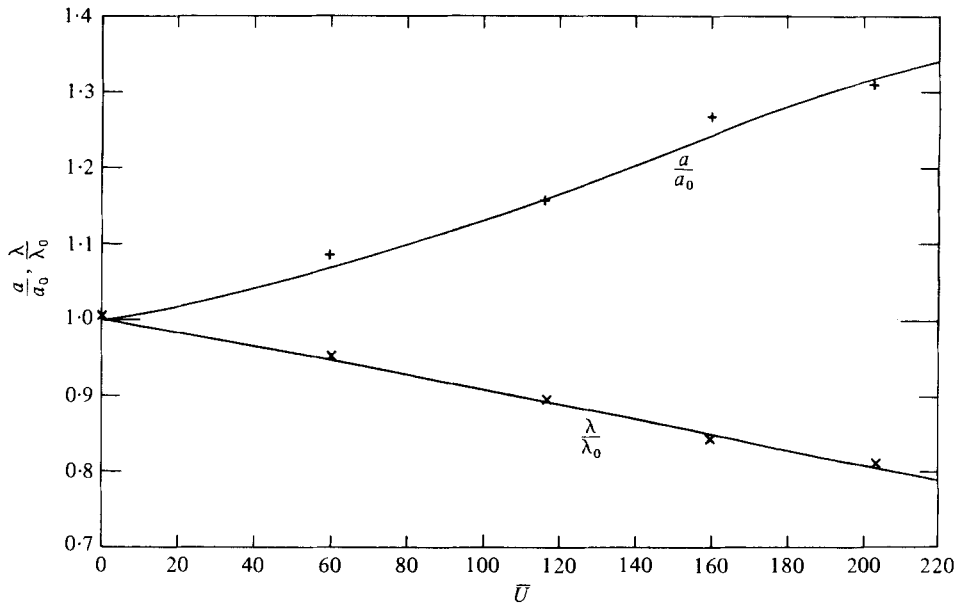


FIGURE 8. The predicted and experimentally obtained values of the non-dimensional wave amplitude a/a_0 and wavelength λ/λ_0 plotted against the mean current \bar{U} (measured in mm s⁻¹). The data is given in table 2. —, the theoretical curve; x, experimentally measured wavelengths; +, experimentally measured wave amplitudes.

The errors between theory and experiment take two forms. The first is the experimental error mentioned above and the second is the error introduced by approximating the current and the wave properties by their mean irrotational equivalents and assuming that the flow properties are slowly varying. The experimental error can be quantified to be accurate within 1% of the measured quantity; the remaining errors must be due to the mean flow and slowly-varying approximations. Taking this into consideration the accuracy obtained in table 2 and figure 8 using the mean flow and slowly varying approximation is surprisingly good.

6. Conclusions

Good agreement has been shown to exist between the predictions of a numerical model and experimentally measured values of the wavelength and velocity profiles associated with a linear wavetrain interacting with a steady current containing an arbitrary distribution of vorticity. Surprisingly good agreement has also been found between the measured wavelengths and those predicted by the interaction between a linear irrotational wavetrain and an adverse depth-independent current having a value equal to the mean of the measured current profile. The success of the mean flow irrotational model is essentially due to the character of the current profiles considered: although the profiles contained strong narrow shear layers near the flume bed and the free surface they were approximately uniform (and hence irrotational) over the remainder of the depth. An approximate estimate indicates that the same is true for the numerical data of Dalrymple (1977) for the condition using a $\frac{1}{7}$ -power-law current, which resembles the profiles of this study. However, Dalrymple's wave is essentially a long wave of finite amplitude, whereas the waves presented here are linear and nearly deepwater in character.†

The amplitude variation as a function of the mean depth-averaged current was predicted using a slowly varying approach and a comparison then made between theory and experiment. The degree of agreement was surprisingly good, especially as the theoretical formula required two approximations in its derivation. The first of these replaced the rotational current by its irrotational mean value and assumed the flow to be irrotational; the accuracy of this approximation was already known from previous velocity and wavelength measurements. Secondly, a slowly varying regime was assumed to exist, i.e. the changes in the current properties (which generate the variations in the wave properties) occur over a scale of several wavelengths. In practice, this was not so since changes in the magnitude of the current occurred over a length scale of one wavelength and thus the slowly varying theory was not strictly valid, but still described the amplitude variations very well.

The results of this study suggest two particular topics of research in the field of regular wave-steady current interactions. The first is to consider in more detail the importance of the shear in the current for a linear wave regime. It is expected that the numerical model would still describe the flow very well for currents which vary strongly with depth, whereas the irrotational mean current model would not, owing to the increased importance of the shear. Furthermore the amplitude variations, considered theoretically in a slowly varying regime, would not be expected to be well predicted by the model used here but would probably contain a strong dependence upon the shear and may not be amenable to a simple analytic treatment. The second topic is to extend the existing work on linear waves to include finite-amplitude effects, including study of both the local velocity fields and the slowly varying properties of the flow.

During the period of this research the author was a member of the Department of Civil Engineering, University of Bristol and accordingly wishes to express his gratitude to those members of the Department who offered useful guidance and advice,

† This important analogy between Dalrymple's numerical work and the present experimental study was demonstrated by a referee, to whom the author is grateful.

notably to Dr T. L. Shaw (then a member of staff) and to Mr C. L. Wishart and Mr E. Smith of the Hydraulics Laboratory. The work was financed by the Marine Technology Directorate of the Science Research Council and this too is gratefully acknowledged.

REFERENCES

- BRETHERTON, F. P. & GARRETT, G. J. R. 1968 Wavetrains in inhomogeneous moving media. *Proc. Roy. Soc. A* **302**, 529–554.
- BREVIK, I. & AAS, B. 1980 Flume experiments on waves and currents. *Coastal Engng* **3**, 149–177.
- DALRYMPLE, R. A. 1973 Water wave models and wave forces with shear currents. *Coastal & Ocean. Engng Lab., Univ. of Florida. Tech. Rep.* **20**.
- DALRYMPLE, R. A. 1977 A numerical model for periodic finite-amplitude waves on a rotational fluid. *J. Comp. Phys.* **24**, 29–42.
- EVANS, J. T. 1955 Pneumatic and similar breakwaters. *Proc. Roy. Soc. A* **231**, 457–466.
- FENTON, J. D. 1973 Some results for surface gravity waves on shear flows. *J. Inst. Math. Applic.* **12**, 1–20.
- HOFFEN, J. D. A. VAN & KARAKI, S. 1976 Interaction of Waves and a Turbulent Current. *Proc. 15th Coastal Engng Conf.*, vol. 1, pp. 404–422.
- HUGHES, B. A. & STEWART, R. W. 1961 Interaction between gravity waves and a shear flow. *J. Fluid Mech.* **10**, 385–400.
- JONSSON, I. G., BRINK-KJAER, O. & THOMAS, G. P. 1978 Wave action and set-down for waves on a shear current. *J. Fluid Mech.* **87**, 401–416.
- Longuet-Higgins, M. S. & Stewart, R. W. 1961 Changes in amplitude of short gravity waves on steady non-uniform currents. *J. Fluid Mech.* **10**, 529–549.
- PEREGRINE, D. H. 1976 Interaction of water waves and currents. *Adv. Appl. Math.* **16**, 9–117.
- SARPKAYA, T. 1955 Oscillatory gravity waves in flowing water. *Proc. A.S.C.E. Engng Mech. Div.* **81**, 815.1–815.33.
- SARPKAYA, T. 1957 Oscillatory gravity waves in flowing water. *Trans. A.S.C.E.* **122**, 564–586.
- SHAW, T. L. & HUTCHINSON, R. S. 1978 Assessment of hydrodynamic facilities for research in marine technology. Report submitted to Marine Technology Directorate of U.K. Science Research Council.
- TAYLOR, G. I. 1955 The action of a surface current used as a breakwater. *Proc. Roy. Soc. A* **231**, 466–478.
- THOMAS, G. P. 1979a Water wave-current interactions: a review. In *Mechanics of Wave-Induced Forces on Cylinders* (ed. T. L. Shaw), pp. 179–203. Pitman.
- THOMAS, G. P. 1979b Wave-current interactions: an experimental and numerical study. In *Mechanics of Wave-Induced Forces on Cylinders* (ed. T. L. Shaw), pp. 260–271. Pitman.
- URSELL, F., DEAN, R. G. & YU, Y. S. 1960 Forced small-amplitude water waves: a comparison of theory and experiment. *J. Fluid Mech.* **7**, 33–52.
- WHITHAM, G. B. 1974 *Linear and Non-linear Waves*. Wiley-Interscience.
- YU, Y.-Y. 1952 Breaking of waves by opposing currents. *Trans. Am. Geophys. Union* **33**, 39–41.